

Temperature and Solvent Effects on the Luminescence Spectrum of C₇₀: Assignment of the Lowest Singlet and Triplet States

S. M. Argentine, K. T. Kotz, and A. H. Francis*

Contribution from the Department of Chemistry, The University of Michigan, Ann Arbor, Michigan 48109

Received July 27, 1995[⊗]

Abstract: The temperature, solvent, and concentration dependence of the fluorescence and phosphorescence spectra of C₇₀ in glassy solutions have been examined. Spectra have been recorded over the temperature range 4–200 K. In addition, the AC Stark field modulated phosphorescence and the phosphorescence of ¹³C₇₀ have been recorded and analyzed. The lowest triplet state is identified as a ³E₁' state and the vibronic structure consists primarily of Herzberg–Teller active e₂' modes. The intensity of the electronic origin is comparable to the vibronically induced intensity and is extraordinarily solvent sensitive. The solvent sensitivity exhibited by the spectra is shown to have the same origins as that observed in benzene and pyrene, but is several times greater in magnitude. Analysis of the spectra suggests that two electronic excited states contribute to the observed phosphorescence spectrum.

Introduction

The fluorescence of C₇₀ has been examined in a variety of different solvents and the reported spectra exhibit substantial differences in the number and relative intensity of vibronic features.^{1–8} In particular, the room temperature fluorescence spectra reported by Williams and Verhoeven² and Sun and Bunker³ exhibit prominent intensity differences between the electronic origin and the first vibronic feature in hexane, benzene, toluene, and dichloromethane. Palewska et al.⁴ noted the pronounced difference in intensity between a vibronic feature of their fluorescence spectrum in *n*-hexane at 77 K and the same band in the spectrum reported by Arbogast and Foote⁵ and taken in 3:1 MCH/3-methylpentane glass at the same temperature. Sun et al. have recently reported large variations in the vibronic structure of fluorescence in mixtures of polar and nonpolar solvents.⁹

We have observed similar solvent sensitivity in the phosphorescence spectra of C₇₀ recorded in different solvents at a number of concentrations and temperatures. Both the number of vibronic features and their relative intensity have been observed to change with temperature and solvent. The sensitivity of both the fluorescence and phosphorescence spectra to solvent and temperature has complicated the analysis of the spectra.

In the present work we report a detailed examination of the temperature, solvent, electric field, and isotopic dependence of C₇₀ fluorescence and phosphorescence. The objective of the

study was to identify and differentiate the various processes contributing to the variability of the luminescence spectra of C₇₀.

Experimental Section

Materials. C₇₀ was purchased from SES Corp. The purity of the samples was ascertained by HPLC with UV detection at 287 nm. The Fullsep column used for this purpose has been shown to provide good separation of C₆₀, C₇₀, and C_{n>70} in hexane.¹⁰ The HPLC chromatograms showed only a single C₇₀ component. The purity of the sample materials was estimated to be >98 mol % based on the optical absorbance of fullerenes at 287 nm. ¹³C₇₀ was provided by Prof. Charles Lieber of Harvard University and the preparation is described elsewhere.¹¹

All solutions were prepared by dissolving C₇₀ in sufficient solvent to make ≈10⁻⁴ M stock solutions. The solutions were filtered through a 0.2 μm Teflon filter to remove undissolved, suspended particles. The solutions were diluted and their final concentration determined by absorption spectroscopy using the molar absorptivity of C₇₀ at 488 nm (14500 L/(mol cm)) reported by Williams and Verhoeven.² C₇₀ solutions ranging in concentration from 10⁻⁴ to 10⁻⁶ M were prepared in spectrophotometric grade toluene, methylcyclohexane (MCH), and 3:1 v/v MCH/iodoethane. Photoluminescence measurements were carried out on ≈1-mL aliquots of the sample solutions sealed in 3 mm i.d. Spectrosil quartz tubing. The solutions were degassed by 3 freeze–evacuate–thaw cycles before heat sealing the quartz cells under vacuum.

Instruments. The sealed solution cells were cooled in a Janis 10DT cryostat to temperatures between 200 and 5 K with a flow of cold nitrogen or helium gas. Temperatures below 5 K were obtained by immersion in liquid helium. The temperature of the sample was regulated by a Lake Shore Model 805 controller and measured with a Lake Shore Type DT-470 silicon diode temperature sensor placed in the cooling gas stream within 1 cm of the sample.

Photoluminescence was stimulated by broad-band excitation of the weak, long-wavelength fullerene absorption bands using a high-pressure

(10) Xiao, J.; Savina, M. R.; Martin, G. B.; Francis, A. H.; Meyerhoff, M. E. *J. Am. Chem. Soc.* **1994**, *116*, 9341.

(11) (a) Argentine, S. M.; Francis, A. H. *In Science and Technology of Fullerene Materials*; Bernier, P., Bethune, D. S., Chien, L. Y., Ebbesen, T. W., Metzger, R. M., Mintmire, J. W., Eds.; MRS Symposium Proceedings Series 359; Materials Research Society: Pittsburgh, PA, 1995; pp 221–227. (b) Argentine, S. M.; Francis, A. H.; Chen, C.-C.; Lieber, C. M.; Siegel, J. S. *J. Phys. Chem.* **1994**, *98*, 7350.

* Author to whom correspondence should be addressed.

⊗ Abstract published in *Advance ACS Abstracts*, November 15, 1995.

(1) Shin, E.; Park, J.; Lee, M.; Kim, D.; Suh, Y. D.; Yang, S. I.; Jin, S. M.; Kim, S. K. *Chem. Phys. Lett.* **1993**, *209*, 427.

(2) Williams, R. M.; Verhoeven, J. W. *Chem. Phys. Lett.* **1992**, *194*, 446.

(3) Sun, Y.-P.; Bunker, C. E. *J. Phys. Chem.* **1993**, *97*, 6770.

(4) Palewska, K.; Sworakowski, J.; Chojnacki, H.; Meister, E. C.; Wild, U. P. *J. Phys. Chem.* **1993**, *97*, 12167.

(5) Arbogast, J. W.; Foote, C. S. *J. Am. Chem. Soc.* **1991**, *113*, 8886.

(6) Catalan, J.; Elguero, J. *J. Am. Chem. Soc.* **1993**, *115*, 9249.

(7) Kim, D.; Lee, M.; Suh, Y. D.; Kim, S. K. *J. Am. Chem. Soc.* **1992**, *114*, 4429.

(8) Wang, Y. *J. Phys. Chem.* **1992**, *96*, 764.

(9) Sun, Y.-P.; Ma, B.; Bunker, C. E. *J. Chem. Soc., Chem. Commun.* **1994**, *18*, 2099.

Osram 1 kW xenon arc lamp and a 10 cm path length of 0.162 M CuSO₄ solution that transmits between 340 and 540 nm.¹² The photoluminescence was collected by a large aperture (*f*/4) plano-convex lens system, passed through a Corning 2-63 glass filter to remove scattered excitation wavelengths, and then dispersed with a *f*/4 scanning monochromator (Acton Research Corp. Spectrapro 275). The red fluorescence was detected with a cooled Hamamatsu R375 photomultiplier tube and the IR phosphorescence was detected with a cooled, red-sensitivity-enhanced Hamamatsu R1767 photomultiplier tube. To improve the signal/noise ratio, the emission was modulated with a mechanical chopper, demodulated with a lock-in amplifier (Princeton Applied Research, Model 124), and digitally recorded using a Keithley Model 575 interface.

Stark modulated luminescence spectra were recorded in an unusual configuration. Since line widths and disorder in vitreous media preclude any possibility of observing Stark splittings or accurately measuring Stark shifts, only intensity changes were of interest. Since a homogeneous Stark field was not required, we employed a sharply pointed metal electrode as the Stark electrode. The field gradients produced at the tip are approximately V/r , where V is the applied potential and r is the radius of curvature of the tip. The electrode was a highly polished stainless steel needle affixed to the end of a cryogenic high-voltage cable and suspended in the cryostat. The field gradient at the tip was 30–40 kV/cm. The focussed 515-nm output of a Coherent Innova argon ion laser provided optical excitation of a small volume at the tip of the Stark electrode. The sample for Stark field modulated spectra consisted of C₇₀ in a dilute polystyrene matrix that was applied directly to the end of the needle electrode.

The Stark field generator consisted of a conventional 100-W audio-frequency amplifier driving two cascaded step-up transformers to produce a potential of 5–6 kV at 30–3000 Hz. The input signal for the generator was taken from the reference oscillator of the lock-in amplifier used to detect the Stark modulated signal. The field was typically modulated at 100 Hz and the modulated luminescence detected at 200 Hz.

Results and Discussion

Luminescent States and Selection Rules. C₇₀ has been the subject of numerous quantum chemical studies of its electronic structure. Both semiempirical and *ab initio* calculations predict the HOMO to have a_2'' symmetry in the D_{5h} molecular point group. The LUMO and LUMO+1 belong to the e_1'' and a_1'' irreducible representations and are sufficiently close in energy that their ordering is uncertain.^{13,14} Therefore, two possibilities must be considered for the electronic configuration of the lowest singlet and triplet excited states: $(a_2'')^1(e_1'')^1$ and $(a_2'')^1(a_1'')^1$. The first configuration corresponds to a E_1' state and the second to an A_2' state. The relative ordering of the triplet states may not be the same as the singlet states due to differences in electron correlation between the two configurations. Also, the degeneracy of the orbital doublet state may be removed by a Jahn–Teller distortion. The presence of a Jahn–Teller distortion has been inferred from the triplet EPR spectra of photoexcited C₇₀.¹⁵

Transitions between the A_1' ground state and the A_2' state are electric dipole forbidden but may be vibronically induced by Herzberg–Teller active vibrations. In the Herzberg–Teller treatment¹⁶ of vibronically induced electric dipole transitions, the ground and excited state adiabatic wave functions are expanded in terms of crude Born–Oppenheimer electronic wave functions with fixed equilibrium nuclear coordinates (Q^0) and coefficients that depend explicitly on the nuclear coordinates

(Q). For the α th electronic state,

$$\varphi_\alpha(q, Q) = \sum c_{\alpha j}(Q) \varphi_j^0(q) \quad (1)$$

For each electronic state α , only the $\alpha = j$ coefficient has appreciable magnitude, approximating unity. The coefficients $c_{\alpha j}(Q)$ are given by first-order perturbation theory as,

$$c_{\alpha j}^k R(Q_k) = \langle \varphi_\alpha^0 | \partial \mathcal{H} \partial Q_k | \varphi_j^0 \rangle Q_k / (E_\alpha^0 - E_j^0) \quad (2)$$

where \mathcal{H} is the electronic Hamiltonian and Q_k is the k th normal coordinate. From eqs 1 and 2, the following approximate result is obtained for the expectation value of the transition dipole moment between the ground ($\alpha = 0$) and the α th excited electronic state,

$$M_{0\alpha} \approx (M_{0\alpha})_0 + \sum c_{\alpha j}^k M_{0j}^0 + \sum (c_{0i}^k)^* M_{i\alpha}^0 \quad (3)$$

The summed indices (i, j) run over all states except $j = \alpha$ and $i = 0$. The first term is the transition dipole moment for the equilibrium molecular geometry and is usually dominant for electric dipole allowed transitions. It is responsible for the intensity of the electronic origin. The terms in the summations represent the mixing of electric dipole allowed states into the ground and excited electronic states by nuclear vibrations. Terms in the summations must be considered when the first term vanishes, as for transitions forbidden by molecular symmetry, or is unusually small (overlap forbidden or angular momentum forbidden transitions). Transitions induced by terms in the summation are displaced energetically from the electronic origin by energies $h\nu_j$, where ν_j is the frequency of a normal vibration. In the condensed phase, the Herzberg–Teller expansion (eq 1) should properly be extended to include not only the internal vibrational degrees of freedom but also phonon modes of libration and oscillation of the molecule in its environment. The participation of low-frequency phonon modes leads to a temperature dependence of the transition dipole moment of electric dipole forbidden transitions.

Herzberg–Teller active vibrations are those that transform as the direct product representation of the excited state and at least one component of the dipole moment operator. The active vibrations for the $A_2' \leftrightarrow A_1'$ transition of C₇₀ are of e_1' or a_1'' symmetry. The $E_1' \leftrightarrow A_1'$ transition is electric dipole allowed with a transition dipole moment perpendicular to the 5-fold axis. Vibrations of symmetry a_1' , a_2' , and e_2' may be Franck–Condon or Herzberg–Teller active in the spectrum of the E_1' state. Since the E_1' state is unstable with respect to a Jahn–Teller distortion along the e_2' coordinate, these modes may also be Jahn–Teller active. Irrespective of the selection rules based on molecular symmetry, the HOMO–LUMO transition of C₇₀ is expected to be weak because the excited states are analogous to the Platt L-type state of a planar, catacondensed aromatic hydrocarbon and thus forbidden by selection rules based on the conservation of electronic angular momentum.¹⁷ Angular momentum may be a particularly good quantum number for highly symmetrical fullerenes.¹¹

Phosphorescence. The phosphorescence spectrum of C₇₀ in MCH glassy solution is shown in Figure 1. The spectrum, which exhibits numerous vibronic features but lacks a dominant high-energy electronic origin, has the characteristic appearance of a vibronically induced transition. We discard the possibility of a Franck–Condon forbidden transition as unlikely for a one-electron excited state of a very large molecule. The difficulty presented by the vibronic analysis of the spectrum is that a

(12) Kasha, M. *J. Opt. Soc.* **1948**, 929.

(13) Baker, J.; Fowler, P. W.; Lazzarotti, P.; Malogoli, M.; Zanasi, R. *Chem. Phys. Lett.* **1991**, 184, 182.

(14) Fowler, P. W.; Lazzarotti, P.; Malogoli, M.; Zanasi, R. *Chem. Phys. Lett.* **1991**, 179, 174.

(15) Terazima, M.; Sakurada, K.; Hirota, N.; Shinohara, H.; Saito, Y. *J. Phys. Chem.* **1993**, 365, 398.

(16) Herzberg, G.; Teller, E. *Z. Phys. Chem.* **1933**, B21, 410.

(17) Platt, J. R. *J. Chem. Phys.* **1949**, 17, 484.

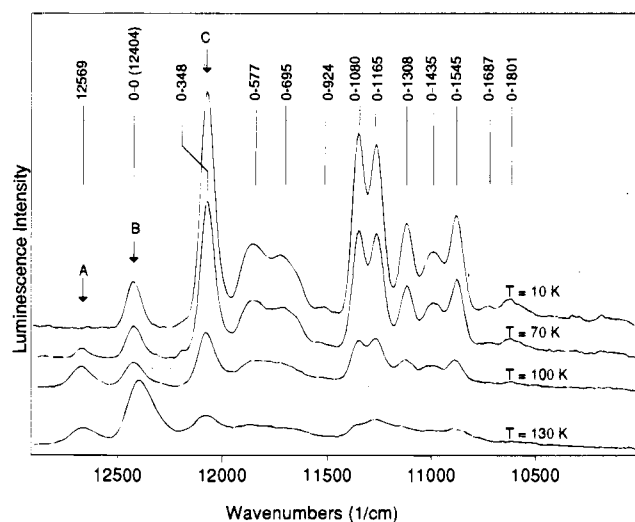


Figure 1. Temperature variation of the C_{70} phosphorescence spectrum in MCH.

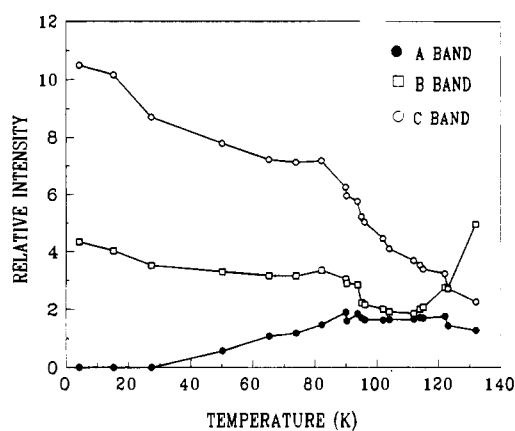


Figure 2. Temperature dependence of the peak intensity of bands A, B, and C.

satisfactory analysis, in terms of the observed ground state vibrational frequencies, cannot be achieved based upon band A as the electronic origin. For this reason it is necessary to consider alternatives for electronic origin assignments based on the temperature and solvent sensitivity of the bands designated A, B, and C in Figure 1.

Temperature Dependence. The temperature variation of the phosphorescence spectrum in MCH glass has been examined in detail by recording the spectrum at approximately 10 K intervals between about 4 and 130 K. Figure 1 shows selected spectra recorded over this range. Above 130 K the MCH glass passes through the glass transition and the phosphorescence is strongly quenched, although fluorescence persists at 300 K. Cooling to 4 K produces only a slight decrease in line width but causes significant changes in the relative intensity of the vibronic features. The thermally induced changes in the phosphorescence spectrum may be represented by the behavior of the three bands designated A, B, and C in Figure 1. The peak intensities of bands A, B and C are plotted as a function of temperature in Figure 2. As the temperature is decreased from 130 K the intensity of the A band remains nearly constant until about 90 K, at which point the intensity decreases rapidly. Band A could not be detected below about 20 K. Band B is the most intense feature of the spectrum near the glass transition at 130 K. Upon cooling the intensity of band B passes through a minimum at about 90 K and the peak shifts slightly

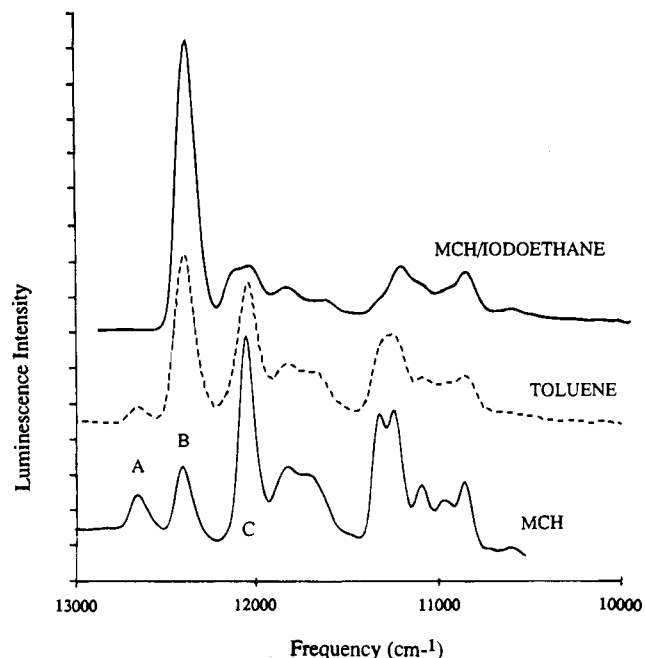


Figure 3. The phosphorescence spectrum of C_{70} in MCH and toluene recorded at 77 K and in a 3:1 MCH/iodoethane mixture recorded at 4 K.

($\approx 30 \text{ cm}^{-1}$) to higher energy. It has been demonstrated by examination of the triplet EPR spectrum that the C_{70} acquires rotational freedom about the long molecular axis before the matrix liquefies¹⁵ and the temperature behavior of the peak may, in part, reflect these dynamics. Band C (together with all remaining bands) increases monotonically as the glass is cooled from 130 to 4 K.

Solvent Effects. Figure 3 shows the phosphorescence spectra of $10^{-5} \text{ M } C_{70}$ in low-temperature glassy solutions of MCH, toluene, and 3:1 MCH/iodoethane. It was necessary to employ MCH in combination with iodoethane in order to promote formation of a good glass. C_{70} is sparingly soluble in many hydrocarbon solvents and has been shown to associate in solution.¹⁸ To identify possible contributions to the phosphorescence spectrum from C_{70} clusters, the spectra were examined as a function of concentration from approximately 10^{-5} M , the limit of solubility in MCH, to the lowest concentration at which satisfactory spectra could be obtained (10^{-6} M). Although the overall luminescence was weaker in the most concentrated solutions, no changes in the relative intensity of the vibronic features were observed over the concentration range studied. Neither were the relative intensities of the vibronic bands sensitive to the cooling rate with which the glassy solutions were prepared. If association occurs, the chief effect appears to be quenching of the luminescence.

The luminescence spectra of C_{70} in the glassy solutions studied are notable for the narrow line widths of the vibronic bands. The typical line width of C_{70} emission at 77 K is $\approx 50 \text{ cm}^{-1}$ (fwhm), compared with $\approx 200 \text{ cm}^{-1}$ for a nonpolar, aromatic hydrocarbon in the same matrices at the same temperature. The line shapes are approximately Gaussian and the line widths provide a measure of the strength of solvent-solute interactions. The narrowness is likely a consequence of the absence of a permanent molecular dipole moment or dipolar bonds, as well as the size and rigidity of the molecular framework. In addition, narrower line widths may result from the decrease in the magnitude of the Onsager solvent reaction field averaged over a large solvent cavity. Polarity plays an

important role in the solvent/solute interaction and the solvents with greater dielectric constants perturb the electronic states of the solute to a greater extent. MCH is the least polar of these solvents and iodoethane is the most polar.

Given the weakness of solute-solvent interactions implied by the line widths, it is interesting that the intensities of the vibronic bands are so strongly affected by the solvent. This is a clear demonstration of the axiom that transition probability of forbidden transitions is more sensitive to perturbation of the electronic wave function than the state energies. The most striking effect of increasing solvent polarity is the increase in the intensity of the B band relative to the other features of the spectrum. The ratio of the intensity of the B band to the C band increases by an order of magnitude as the dielectric constant of the solvent increases from 2.02 D in MCH to 7.82 D in iodoethane. Similar behavior of the fluorescence of C_{70} has been reported by Sun et al.⁹

Relaxation Time. The luminescence intensity of band A has a different relaxation time than that of bands B and C, which decay at the same rate. The lifetime of the B and C bands, determined by exciting the sample with a 20- μ s xenon flash lamp, was found to be ≈ 100 ms in MCH at 77 K. The lifetime of the A band was less than the duration of the flash and was not determined. In addition, when phosphorescence spectra were recorded while modulating the excitation source between 100 and 1000 Hz, the difference between the relaxation rate of the A band and the other spectral features was revealed by changes in the relative intensity of the modulated emission.

Isotope Shifts. The phosphorescence spectrum of $^{13}C_{70}$ was measured in MCH at 77 K and the isotope frequency shifts of the vibronic features determined. The peak positions in the spectrum of C_{70} and $^{13}C_{70}$ were determined to high accuracy by recording the spectra with the emission of a low-pressure rubidium discharge lamp superimposed. The rubidium emission spectrum has several long wavelength lines that nearly coincide with the A, B, and C bands and so provide an accurate calibration. We estimate that the band frequencies were measured to ± 5 cm^{-1} .

All of the peaks in the $^{13}C_{70}$ spectrum are shifted to higher energy with respect to the C_{70} peaks due to the relative change in the vibrational zero-point energies of the ground and excited states. But the isotopic frequency shifts suggest that the A band does not arise from the same electronic state as the B and C bands. Since the molecule contains only carbon, the positions of the $^{13}C_{70}$ bands can be computed from the positions of the C_{70} phosphorescence bands by the following relation:

$$\Delta\nu_j^{(13)} = (12/13)^{1/2} \Delta\nu_j^{(12)} \quad (4)$$

where $\Delta\nu_j^{(13)}$ is the energy difference between the j th vibronic band of $^{13}C_{70}$ and the origin of $^{13}C_{70}$ phosphorescence, and $\Delta\nu_j^{(12)}$ is the energy difference between the j th vibronic band of C_{70} and the origin of C_{70} phosphorescence. If the A band of the C_{70} and $^{13}C_{70}$ spectra is chosen as the electronic origin, the deviation of the observed vibronic band positions from those predicted by eq 4 shows a consistent deviation that is well outside experimental error. If band B is chosen as the electronic origin, the deviations are random and most fall within the estimate of experimental error. The deviations for both choices of origin are plotted in Figure 4 versus band position.

Stark Field Perturbation. For the weak, symmetry and/or angular momentum forbidden luminescence of C_{70} , the principal effect of the AC modulated Stark field is expected to be a modification of the transition probability through the field induced mixing of the excited state electronic wave functions. Since the Stark field will mix states whose direct product

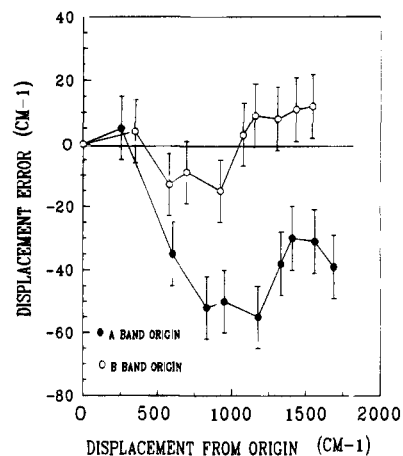


Figure 4. Error between observed and calculated isotope frequency shifts measured relative to band A and band B.

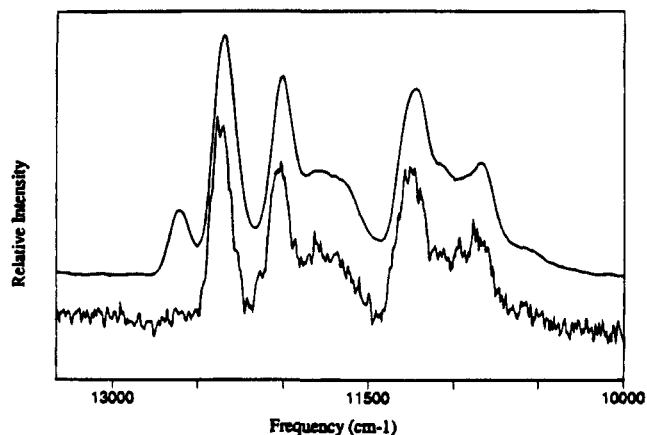


Figure 5. Phosphorescence (upper trace) and AC Stark modulated phosphorescence spectrum (lower trace) of C_{70} in polystyrene matrices at 77 K.

transforms as a vector, dipole forbidden states are mixed with dipole allowed states. Field induced mixing of the molecular electronic wave functions should therefore result in increased luminescence intensity of otherwise forbidden or weakly allowed transitions.

A 100-Hz, 30-kV/cm AC Stark field was used to obtain the modulated phosphorescence spectrum of C_{70} in polystyrene shown in the lower trace of Figure 5. The total sample luminescence is shown in the upper trace. Since the Stark field induced mixing is independent of the sign of the field, application of a bipolar modulation at frequency ω produces a modulation of phosphorescence at 2ω . All of the bands of the phosphorescence spectrum, except the A band, exhibit a modulated emission at 200 Hz. The intensity changes of all affected features are proportional to the intensities observed in the PL spectrum. Since the Stark field affects the electronic portion of the excited state wave function, the contrasting behavior of the A band suggests that it arises from a different electronic state than the B and C bands. Moreover, the similar behavior of the B and C bands indicates that they belong to a common electronic state. These conclusions are consistent with the solvent and temperature dependence of the A, B, and C bands.

Phosphorescence Vibronic Analysis. In view of the A band's distinctive temperature dependence, solvent sensitivity, isotope shift, relaxation time, and Stark spectrum, we conclude that it is due to emission from a higher electronic state. The higher state is not in thermal equilibrium with the lowest emitting triplet at 77 K and is evidently populated by radia-

Table 1

freq (cm ⁻¹)	diff ^c (cm ⁻¹)	analysis ^a	modes ^d	description ^d
Phosphorescence				
1063	1801	0-569-1165		w
		0-358-1447		
10701	1687	0-569-1062		w
		0-358-1313		
10859	1545	0-1565	e ₂ '	s, m
		0-358-1165		
10969	1435	0-1447	e ₂ '	s, m
		0-358-1062		
11096	1308	0-1313	e ₂ '	s, m
11248	1165	0-1165	a ₁ '	s, m
11324	1080	0-1062	e ₂ '	s, m
11480	924	0-358-569		s, w
11709	695	0-701	e ₂ '	sh, m
11827	577	0-569	a ₁ ', e ₁ ''	m
12056	348	0-(348) ^b	e ₂ '	C-band, s, st
12404	0	0-0		B-band
12659				A-band
Fluorescence				
13976	1231	0-1227	e ₂ '	s, m
14138	1069	0-1062	e ₂ '	m
14334	873	0-358-569		sh
14430	777	0-766	e ₂ '	s, m
14543	664	0-674		sh
		0-228-409		
14642	565	0-569	a ₁ ', e ₁ ''	s, st
14805	402	0-409	e ₂ '	s, m
14852	355	0-(348) ^b		
14973	234	0-228	a ₁ '	
15207	0	0-0		β-band
15336				α-band
15606				temp dep

^a Calculated and experimental frequencies, and normal mode descriptions are from ref 20. ^b Calculated value taken from ref 20. ^c Experimental Raman frequencies from ref 20. ^d st = strong, m = medium, w = weak, s = sharp, sh = shoulder.

tionless relaxation from higher lying states. These conclusions are consistent with the results of Levanon et al.,¹⁹ who have observed the co-existence of two triplet states with substantially different spin relaxation times in the EPR spectrum of photo-excited C₇₀. We rule out the possibility that band A is due to phosphorescence from an excited vibrational state of T₁ because no corresponding vibrational feature can be assigned in the ground state. Moreover, the temperature dependence of the relative intensities of the A and B bands is not consistent with a thermally equilibrated excited vibrational state. Unfortunately, there is insufficient information from the experiments performed to permit an assignment of the higher emitting state. We have not been able to identify any other features associated with emission from the higher state, which presumably lie beneath the emission from the lower energy state.

Choosing the B band as an electronic origin results in a good vibrational analysis, predominately in terms of e₂' normal modes (Table 1). C₇₀ has 22 e₂' normal modes, 16 of which have been observed and assigned in the Raman spectrum.²⁰ Five bands are identified as vibronic origins assigned to e₂' modes. In addition, the e₂' modes appear in several combination bands. The prominent B band (0-348 cm⁻¹) has not been observed in the Raman spectrum, but agrees well with the value calculated²⁰ for one of the low-frequency e₂' modes (348 cm⁻¹). All of the features assigned as involving e₂' modes exhibit the same solvent and temperature dependence. Although the e₂' mode is the only Jahn-Teller active mode of the ³E₁' state, its prominence in

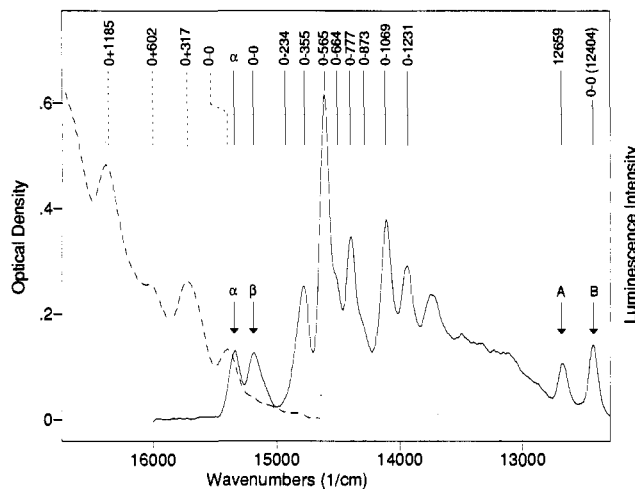


Figure 6. Fluorescence (solid line) and absorption (dashed line) of C₇₀ in MCH at 77 K.

the phosphorescence from this state is evidently due to its Herzberg-Teller activity. No progressions in the e₂' mode could be identified, suggesting that the Jahn-Teller distortion from D_{5h} symmetry is not large.

The vibronic features annotated 0-577 and 0-1165 are assigned to totally symmetric a₁' modes. This assignment is consistent with the solvent and temperature sensitivity of the 0-1165-cm⁻¹ band, which mimics that of the electronic origin (B band). It is of interest that, in nonpolar solvents, the formally allowed electronic origin is substantially weaker than several of the vibronic origins. This occurs because the ³E₁' → ¹A₁' transition, although formally allowed by molecular symmetry, is strongly forbidden by electronic orbital angular momentum selection rules (L → A). In fact, the success of molecule-centered spherical harmonic wave functions in predicting the energetic ordering of the electronic states of C₆₀ suggests that angular momentum may be considered a good quantum number for symmetrical fullerenes.²¹⁻²⁴ Thus, the electronic origin and the totally symmetric vibrations are weak in weakly interacting, noncomplexing solvents that do not reduce the high molecular symmetry. In strongly polar solvents, the reaction field reduces the symmetry and the angular momentum forbiddens of the electronic transition resulting in an increase in the intensity observed for the B band. We may view the phosphorescence as a superposition of two subspectra: (1) an angular momentum forbidden spectrum consisting of the electronic origin and several Franck-Condon active a₁' modes and (2) a vibronically induced spectrum involving Herzberg-Teller active e₂' modes. The two subspectra gain intensity from two different processes, both of which reduce the molecular symmetry.

The role of the solvent reaction field is accentuated in the fullerenes because the magnitude of vibronic coupling matrix elements is smaller than in polyenes and aromatic compounds.²⁵ The largest calculated value of the adiabatic vibronic coupling (defined in eq 2) for C₆₀ is less than 1000 cm⁻¹, whereas polyenes have adiabatic vibronic coupling matrix elements >2000 cm⁻¹.²⁶ This result is probably a consequence of the size of the fullerenes—the vibronic coupling scales with vibrational amplitude and the vibrational energy is distributed over a large number of nuclei. As a result of the decreased

(21) Savina, M. R.; Lohr, L. L.; Francis, A. H. *Chem. Phys. Lett.* **1993**, 205, 200.

(22) Gallup, G. A. *Chem. Phys. Lett.* **1991**, 187, 187.

(23) Ball, D. W. *J. Chem. Ed.* **1994**, 71, 463.

(24) Rioux, F. *J. Chem. Ed.* **1994**, 71, 464.

(25) Negri, F.; Orlandi, G.; Zerbetto, F. *J. Chem. Phys.* **1992**, 97, 6496.

(26) Orlandi, G.; Zerbetto, F.; Zgierski, M. Z. *Chem. Rev.* **1991**, 91, 867.

(19) Levanon, H.; Meiklyar, V.; Michaeli, S.; Gamliel, D. *J. Am. Chem. Soc.* **1993**, 115, 8722.

(20) Jishi, R. A.; Dresselhaus, M. S.; Dresselhaus, G.; Wang, X.-A.; Zhou, P.; Roa, A. M.; Eklund, P. C. *Chem. Phys. Lett.* **1993**, 206, 187.

magnitude of vibronic coupling, the Herzberg–Teller induced spectrum is weaker than observed in smaller molecules, accentuating the role of the solvent in inducing electric dipole transitions.

Fluorescence. Figure 6 shows the fluorescence spectrum of C_{70} in MCH recorded at 77 K. The onset region of the absorption spectrum of C_{70} in MCH glass at 77 K is also shown. Further cooling of the sample results in substantial changes in the relative intensities of the first three peaks, but does not significantly improve the resolution of the spectrum. The solvent sensitivity and temperature dependence of the phosphorescence spectrum are reproduced in the fluorescence spectrum and our analysis follows from this fact. We observe the highest-energy band of the fluorescence system at 77 K in MCH glass at 15336 cm^{-1} (α band) in reasonable agreement with Wang⁸ (15361 cm^{-1}) and Palewska⁴ (15400 cm^{-1}). The α band is similar in its temperature dependence to the A band of the phosphorescence. In the fluorescence spectrum another temperature-dependent band is observed at 15606 cm^{-1} . This band, which is *very* weak at low temperatures and is not visible in Figure 6, increases with temperature and is a prominent

(27) Lianos, P.; Georghiou, S. *Photochem. Photobiol.* **1979**, *30*, 355. **1971**, *44*, 3272.

feature of the room temperature solution fluorescence spectrum. It may correspond to a band reported by Catalán et al.⁶ at 15576 cm^{-1} in the fluorescence spectrum of C_{70} in cyclohexane at room temperature. The bands at 15606 and 15336 cm^{-1} (α band) are assigned to emission from an excited state(s). The 15606 cm^{-1} band is likely a vibrational “hot” band; the α band is believed to be analogous to the A band in phosphorescence whose temperature dependence it mimics.

The band at 15207 cm^{-1} (β band) is analogous to the B band in phosphorescence and is assigned as the electronic origin of the ${}^1E_1' \rightarrow {}^1A_1'$ fluorescence. The vibronic analysis given in Table I is in terms of e_2' modes forming vibronic origins. Many of the active modes are the same as those observed in phosphorescence. In polar solvents, the β band increases in intensity relative to the vibronically induced spectrum. The behavior is completely analogous to that observed in phosphorescence and is an example of the Ham effect in benzene.

Acknowledgment. The authors would like to acknowledge support for this research from the National Science Foundation (DMR 8818371).

JA952527V